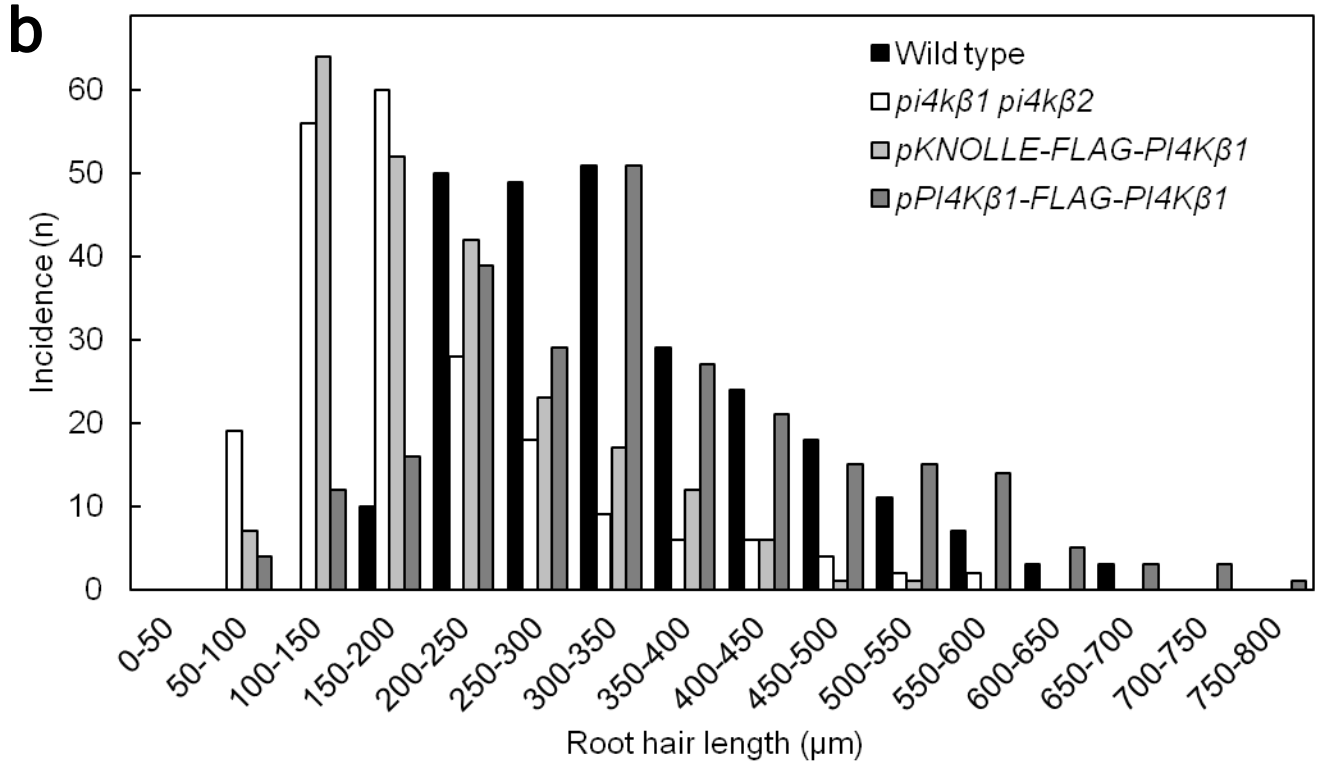


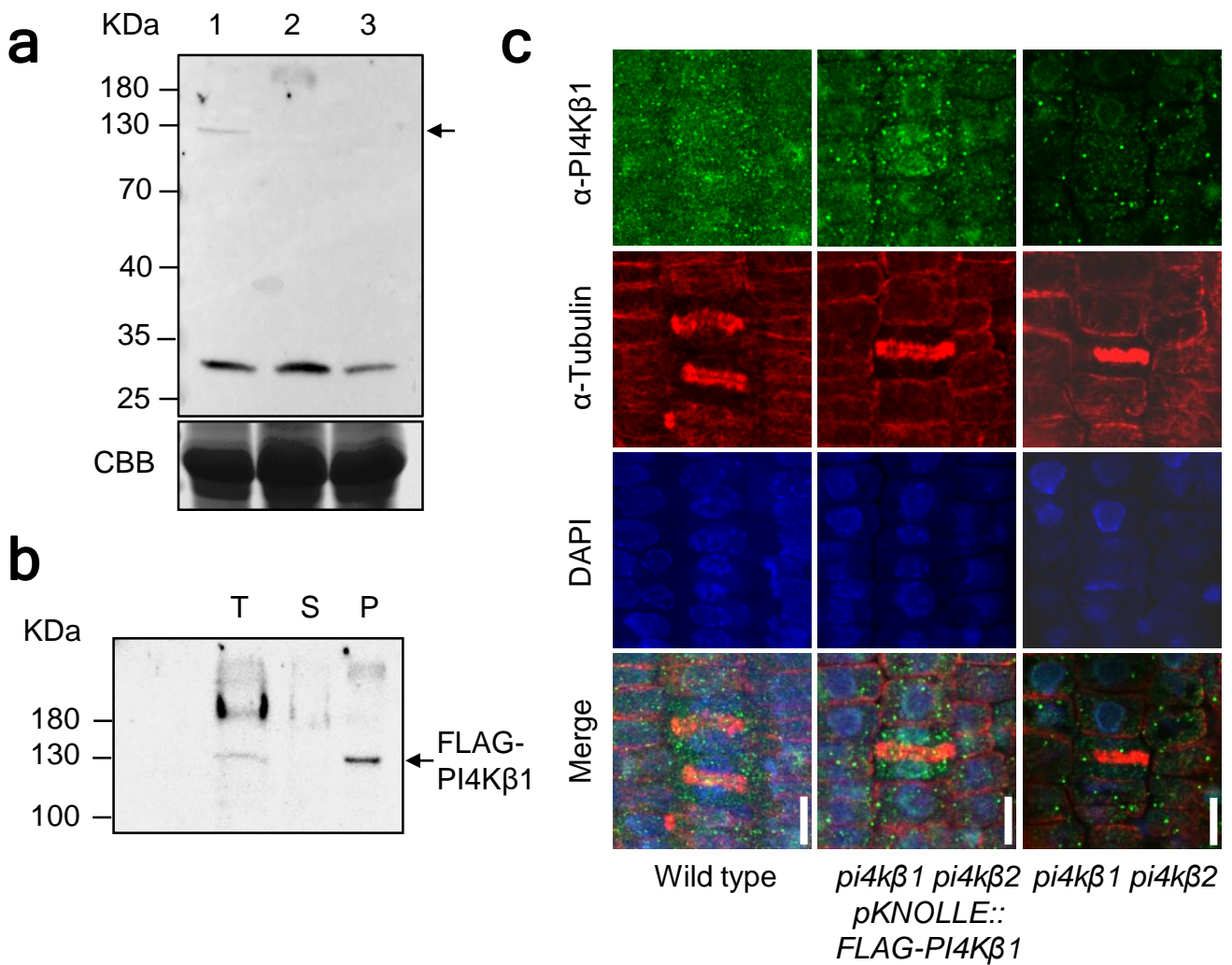
## **Appendix**

### **Table of contents**

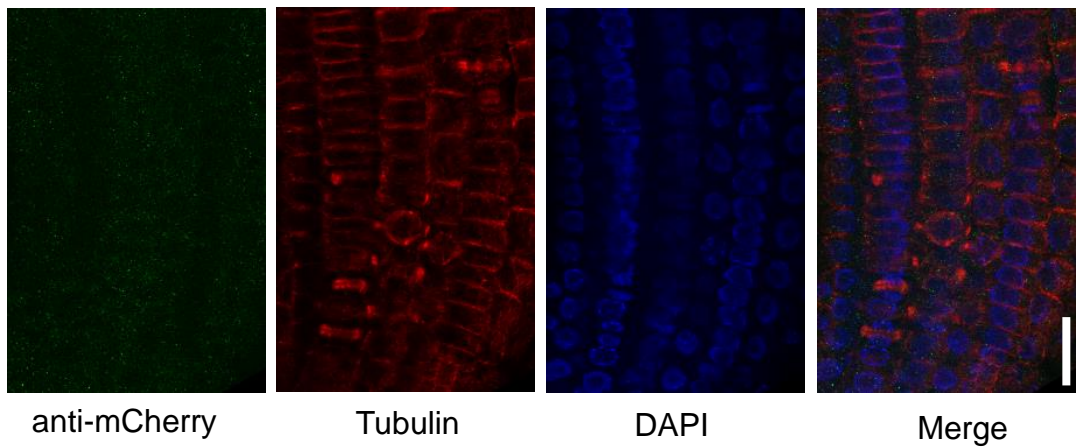
	page
Appendix Figure S1	1
Appendix Figure S2	2
Appendix Figure S3	3
Appendix Figure S4	4
Appendix Figure S5	5
Appendix Figure S6	6
Appendix Figure S7	7
Appendix Figure S8	8
Appendix Figure S9	9
Appendix Figure S10	10
Appendix Table S1	11



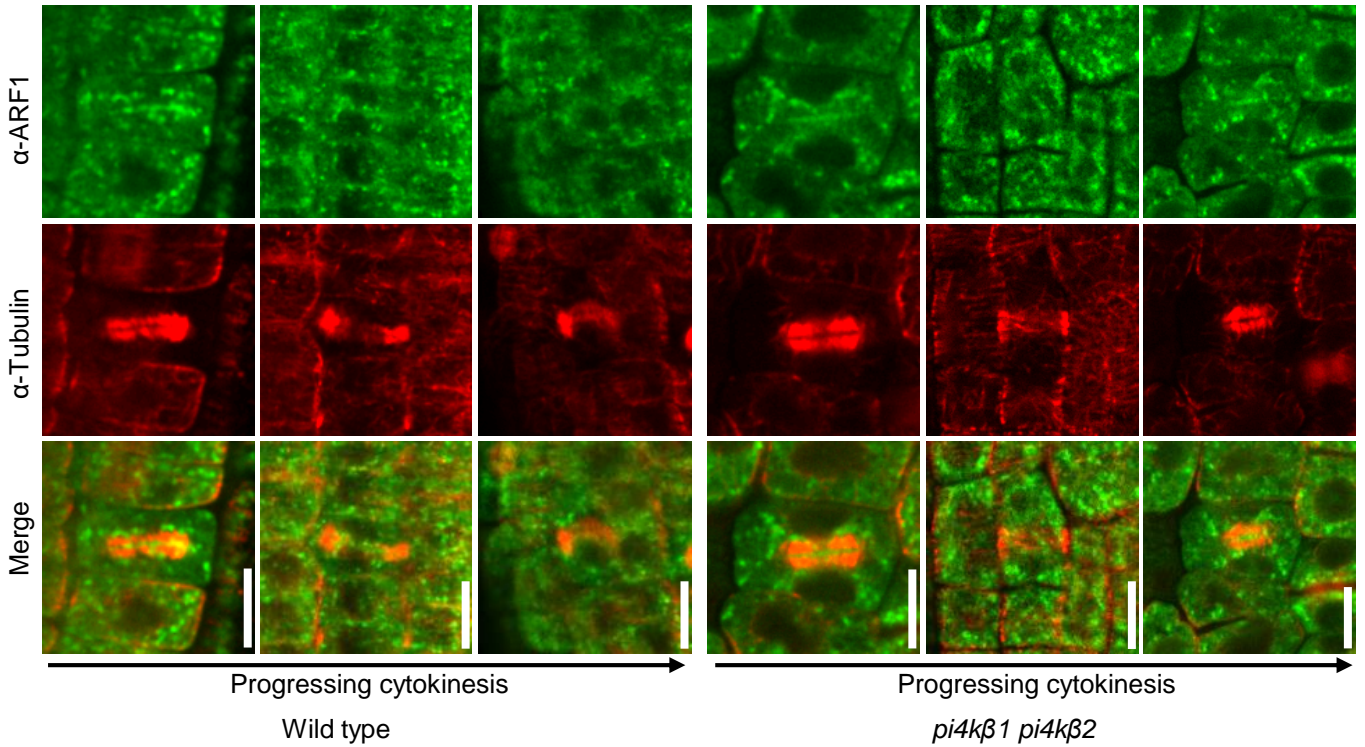
**Appendix Figure S1. Rescue of cytokinetic but not other defects of the Arabidopsis *pi4kβ1 pi4kβ2* phenotype by a FLAG-PI4Kβ1 fusion expressed under KNOLLE cis-regulatory sequences.** To test whether or not PI4Kβ1 functions specifically during cytokinesis, a FLAG-PI4Kβ1 fusion was expressed in *pi4kβ1 pi4kβ2* double mutants from the *pKNOLLE* promoter, which is only active during cytokinesis. Expression rescued cytokinetic but not other defects of the double mutant, suggesting that PI4Kβ isoforms have functions outside cytokinesis. (a) Transgenic lines and controls, as indicated. 50-day-old plants are shown. See also Fig. 1. Scale bar, 10 cm. (b) Quantification of root hair lengths from 4-day-old seedlings. Root hair lengths of double mutant plants expressing the *pKNOLLE*-driven *FLAG-PI4Kβ1* did not differ from those of the double mutants ( $p < 0.272$ ) according to a two-tailed Student's *t*-test, but were significantly different from root hair lengths observed in wild type ( $p < 0.0001$ ) according to a two-tailed Mann-Whitney *U*-test or from fully complemented double mutants expressing *FLAG-PI4Kβ1* from the intrinsic *pPI4Kβ1* promoter ( $p < 0.0001$ ) according to a two-tailed Mann-Whitney *U*-test (wild type,  $n = 255$ , 12 roots; *pi4kβ1 pi4kβ2*,  $n = 210$ , 11 roots; *pKNOLLE:FLAG-PI4Kβ1*,  $n = 225$ , 12 roots; *pPI4Kβ1-FLAG-PI4Kβ1*,  $n = 255$ , 11 roots).



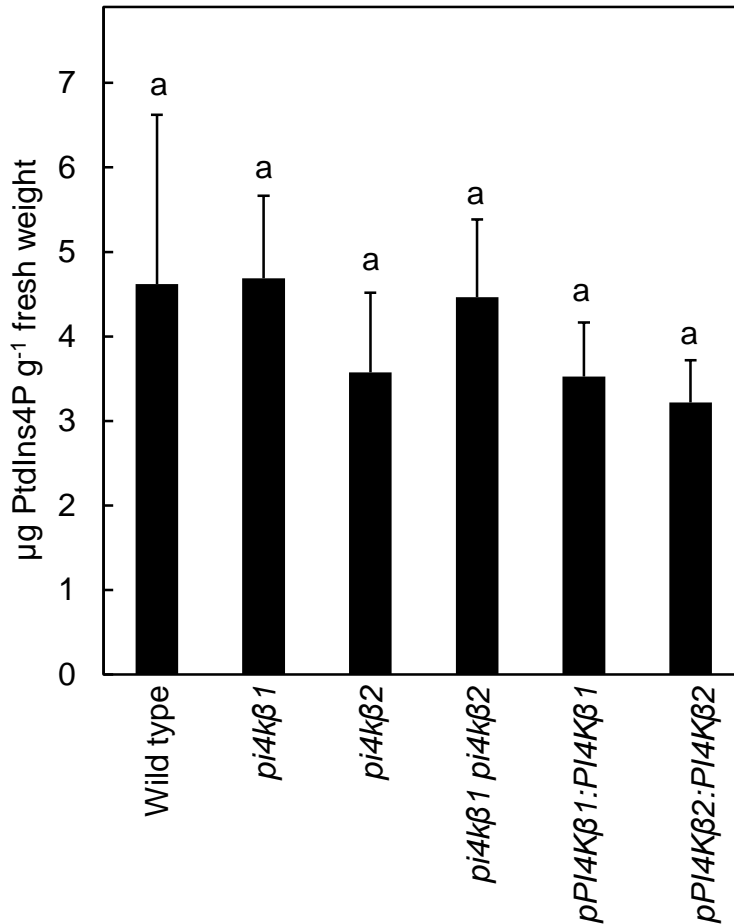
**Appendix Figure S2. Controls for immunodetection experiments.** (a) Characterization of the anti-PI4Kβ1 antibody. 100 μg protein was loaded. Ribulose-1,5-bisphosphat-carboxylase/-oxygenase (RuBisCO) was used as a loading control. CBB: Coomassie Brilliant Blue staining. Lane 1, wild type; lane 2, *pi4kβ1* single mutant; lane 3, *pi4kβ1 pi4kβ2* double mutant. Arrow, PI4Kβ1. Note, the unspecific band at around 30 kDa. (b) Immunodetection of *pPI4Kβ1::FLAG-PI4Kβ1* expressed in the *pi4kβ1 pi4kβ2* double mutant using the anti-PI4Kβ1 antibody. Protein extracts were prepared from *A. thaliana pi4kβ1 pi4kβ2* double mutants expressing *FLAG-PI4Kβ1* driven by the intrinsic *pPI4Kβ1* promoter. The total protein extracts (T) were subjected to centrifugation at 100,000 x g to obtain soluble (S) and a particulate membrane fraction (P). FLAG-PI4Kβ1 was detected in the membrane fraction. Arrowhead, FLAG-PI4Kβ1. (c) No immunofluorescence detection of endogenous Arabidopsis PI4Kβ1 protein using the anti-PI4Kβ1 antibody. Detection was attempted in wild type controls, transgenic *pi4kβ1 pi4kβ2* double mutants expressing FLAG-PI4Kβ1 from the *pKNOLLE* promoter and in *pi4kβ1 pi4kβ2* double mutant controls, as indicated. Images are from whole-mount immunostaining of five-day-old roots using anti-PI4Kβ1 (green), anti-tubulin (red), and DAPI (blue). Note, anti-PI4Kβ1 antiserum showed unspecific signals in *pi4kβ1 pi4kβ2* double mutants, and did not detect PI4Kβ1 protein in wild type or *pKNOLLE::FLAG-PI4Kβ1* plants. Images are representative for n ≥ 55 cells from ≥ 12 roots. Scale bars, 10 μm.



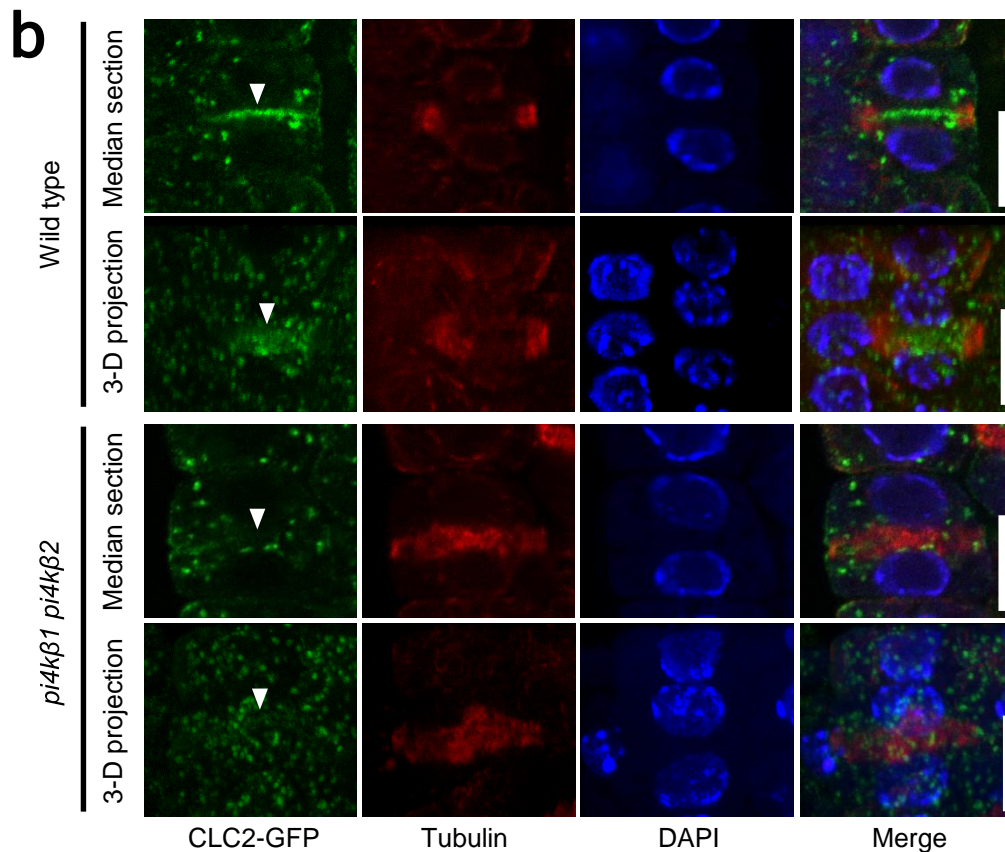
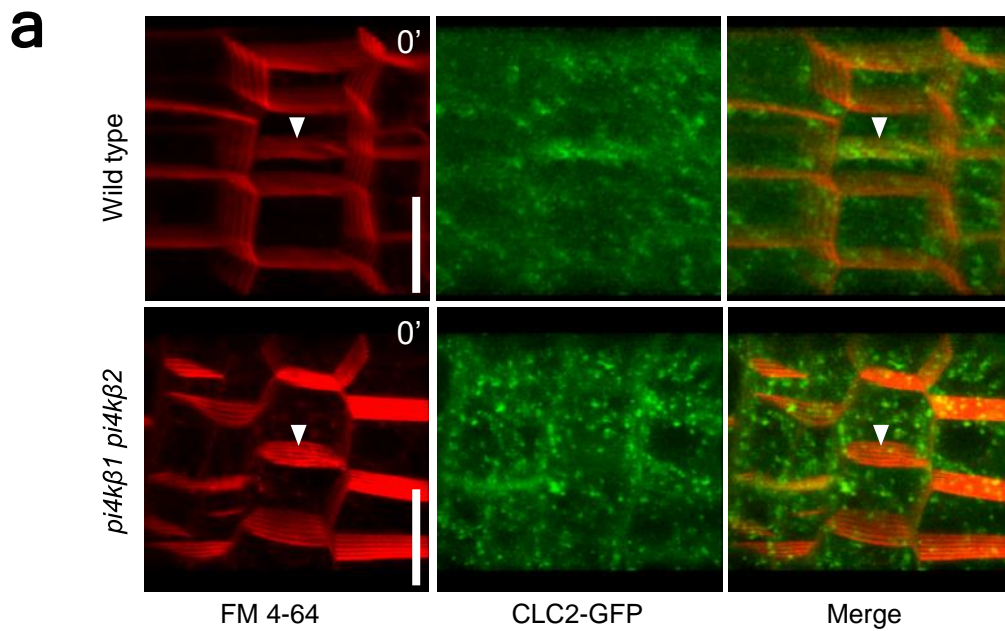
**Appendix Figure S3. Characterization of the anti-mCherry antibody in Arabidopsis roots.** This control was performed to test whether the anti-mCherry antiserum would detect any endogenous Arabidopsis proteins. Immunofluorescence of five-day-old wild type roots was performed using anti-mCherry and anti-tubulin (red) antisera, costained with DAPI (blue). The anti-mCherry antibodies did not cross react with proteins of wild type plants (left panel). Scale bar, 20  $\mu\text{m}$ .



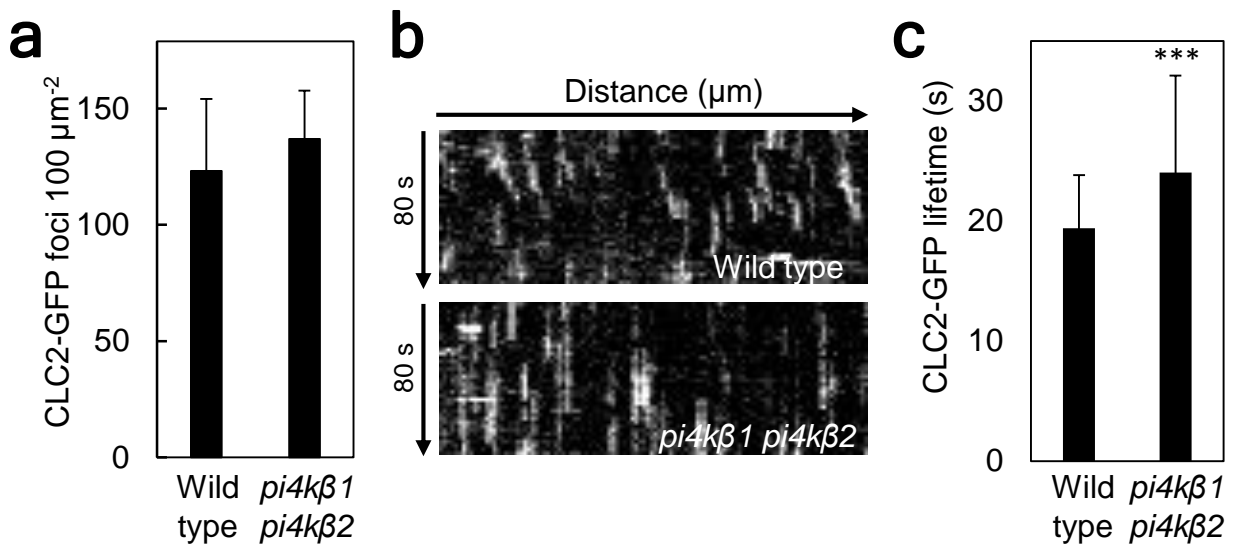
**Appendix Figure S4. Localization of ARF1 is not affected at the cell plate in cytokinetic cells of Arabidopsis *pi4kβ1 pi4kβ2* double mutants.** Five-day-old seedlings were subjected to immunostaining using anti-tubulin (red) and anti-ARF1 (green) antibodies. ARF1 localization was unaffected in cytokinesis of *pi4kβ1 pi4kβ2* double mutants. Images are representative for  $n \geq 40$  cells from 12 roots for each stage of either genotype. Scale bars, 10  $\mu\text{m}$ .



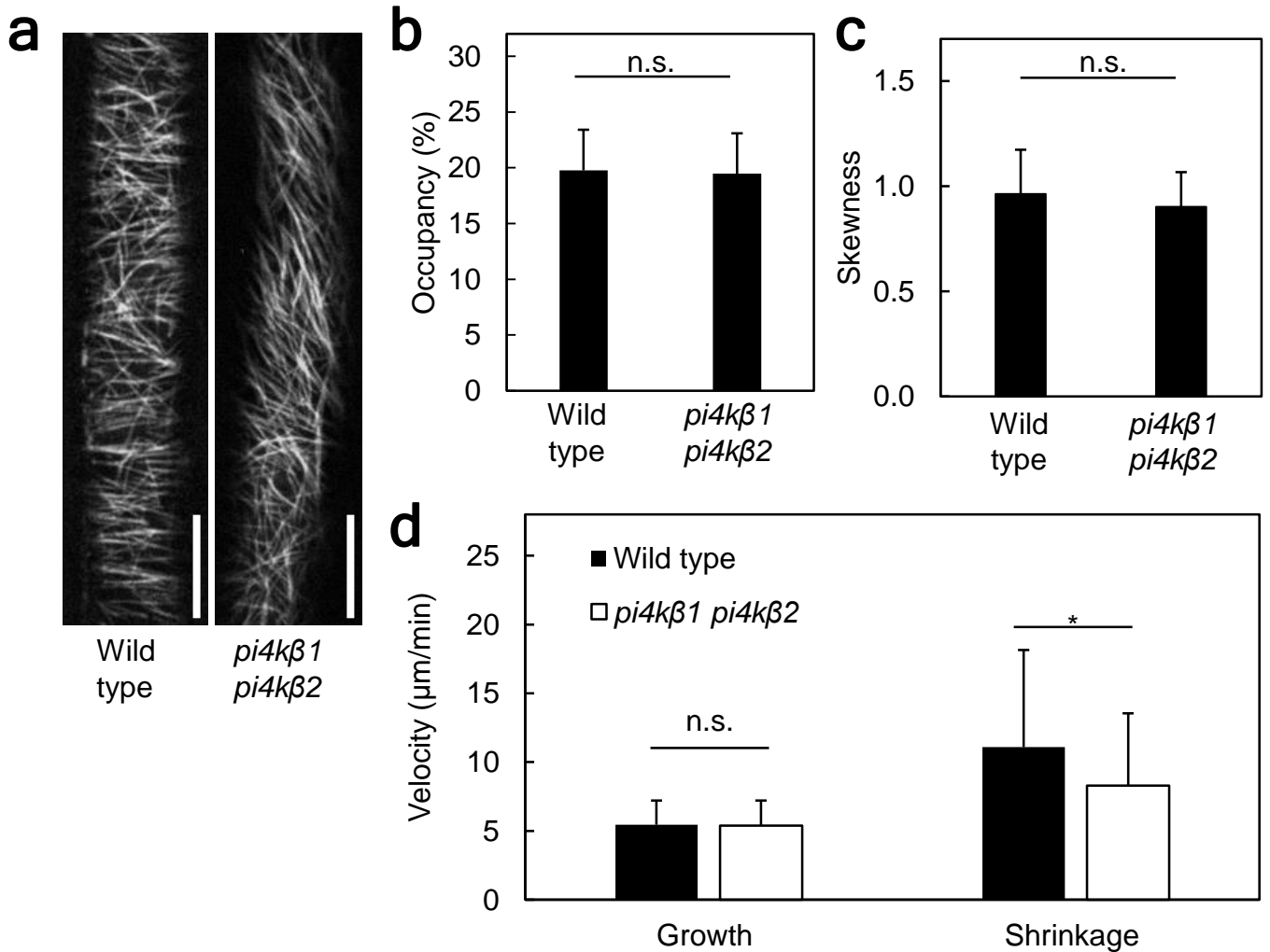
**Appendix Figure S5. Unchanged global PtdIns(4)P levels in the Arabidopsis *pi4kβ1 pi4kβ2* double mutant.** Two-week-old seedlings were subjected to PtdIns(4)P analysis by combined thin-layer-chromatography and gas-chromatography. No differences in PtdIns(4)P were detected according to a one-way ANOVA with post-hoc Tukey HSD with 95% confidence interval between wild type controls, *pi4kβ1* or *pi4kβ2* single mutants, the *pi4kβ1 pi4kβ2* double mutant, or *pi4kβ1 pi4kβ2* double mutants complemented with either *PI4Kβ* gene under their respective intrinsic promoters. Data represent the mean ± SD from three replicates for each genotype.



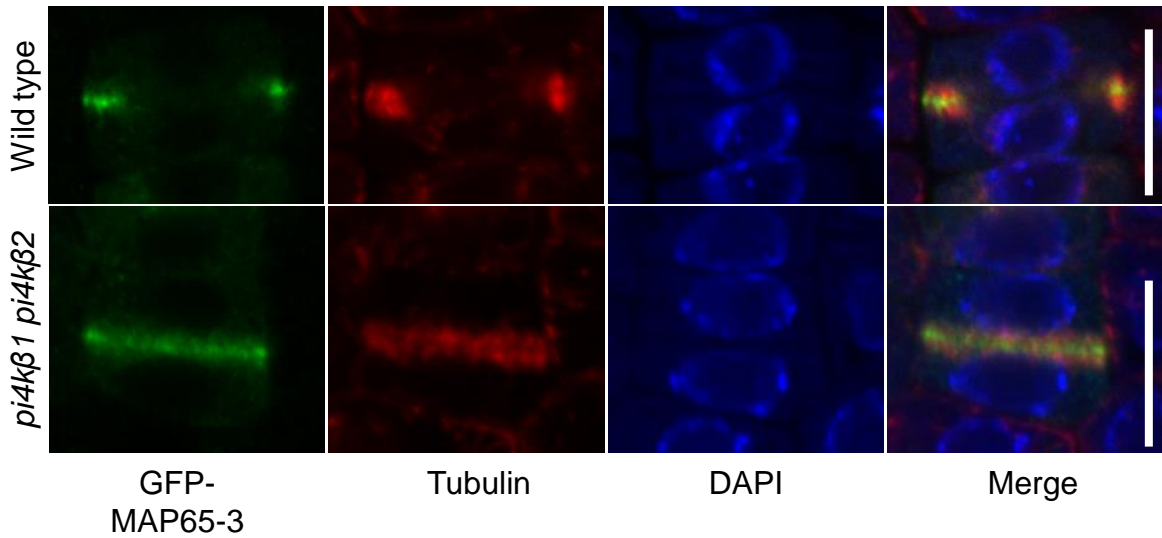
**Appendix Figure S6. Altered recruitment of CLC2 at the cell plate of wild type controls and the *Arabidopsis pi4kβ1 pi4kβ2* double mutant.** CLC2 was detected at the cell plate of root meristem cells of five-day-old seedlings by either live cell imaging (a) or by immunodetection. (a) 3-D projections of t0 from Fig. 4. CLC2-GFP was already recruited to the cell plate (arrowheads) in wild type, whereas the marker was still absent in the *pi4kβ1 pi4kβ2* double mutant. Scale bars, 10 μm. (b) Immunofluorescence of a CLC2-GFP marker (green) and microtubules (red), costained with DAPI (blue). Median confocal sections and 3D projections are both shown, as indicated. Note the reduced CLC2-GFP signal at the cell plates (arrowheads) and the ectopically stabilized phragmoplast in the *pi4kβ1 pi4kβ2* double mutant. The images are representative for ≥ 15 cells for each genotype. Scale bars, 10 μm.



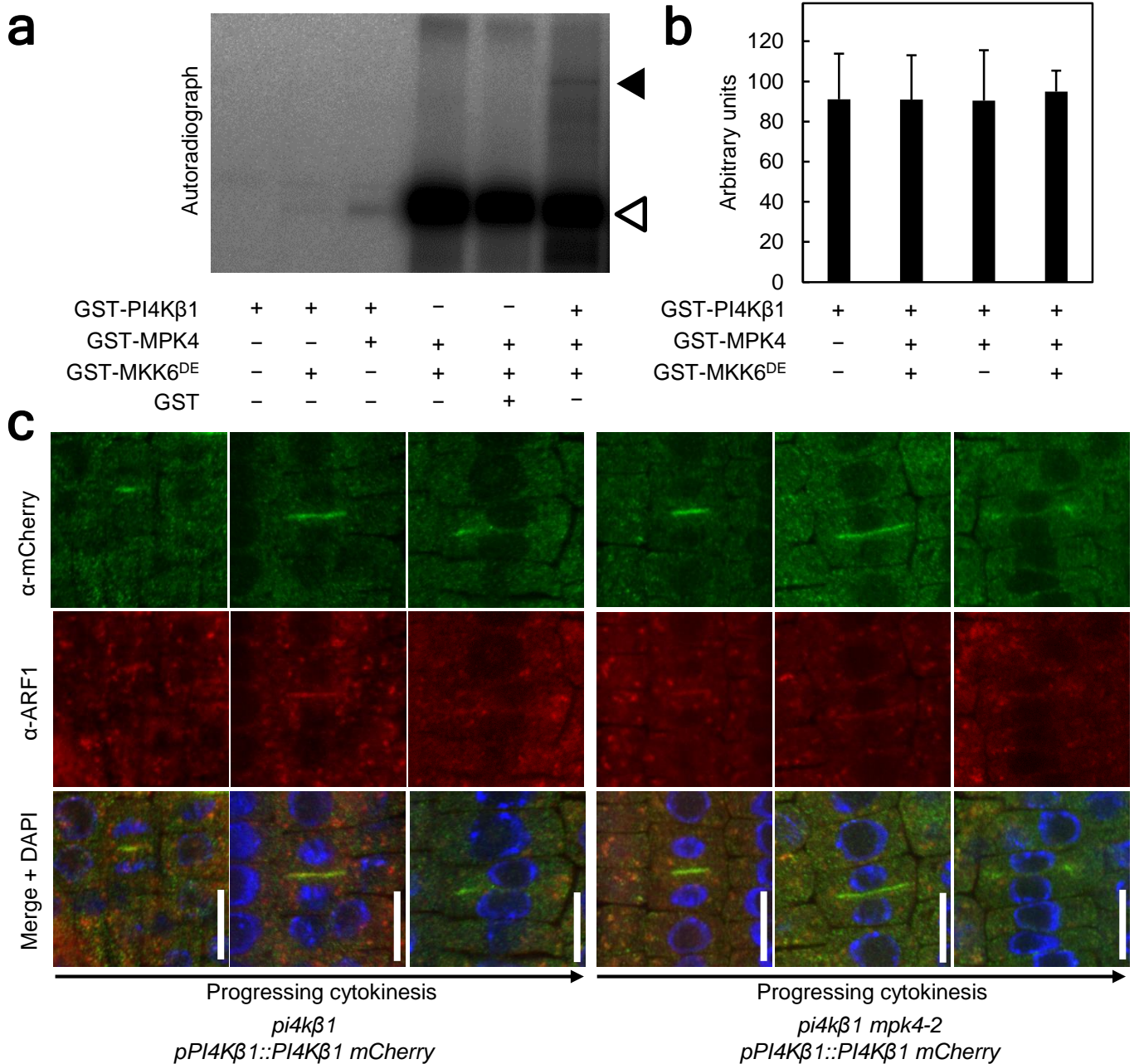
**Appendix Figure S7. Altered clathrin dynamics at the plasma membrane of non-cytokinetic root cells of the *Arabidopsis pi4kβ1 pi4kβ2* double mutant.** Plasma membrane dynamics of CLC2-GFP were recorded by spinning disc microscopy. (a) Area density of CLC2-GFP foci at the plasma membrane in elongating root cells of five-day-old seedlings. No significant difference ( $p < 0.142$ ) was detected between wild type ( $n = 2990$ ) and *pi4kβ1 pi4kβ2* ( $n = 2792$ ) according to a two-tailed Student's *t*-test. (b) Representative kymographs of five-day-old elongating cells showed an increased lifetime of CLC2-GFP foci at the plasma membrane of the *pi4kβ1 pi4kβ2* double mutant cells over that in wild type controls. (c) Quantification of CLC2-GFP lifetime from (b). \*\*\*, a significant difference ( $p < 0.0001$ ) according to a two-tailed Mann–Whitney *U*-test (wild type,  $n = 134$ ; *pi4kβ1 pi4kβ2*,  $n = 130$ ).



**Appendix Figure S8. Altered microtubule dynamics in non-cytokinetic root cells of the *Arabidopsis pi4kβ1 pi4kβ2* double mutant.** The dynamics of cortical microtubular organization were recorded by spinning disc microscopy in cells of the root elongation zone of five-day-old wild type and *pi4kβ1 pi4kβ2* double mutant seedlings expressing the microtubule marker, mCherry-TUA5. (a) Representative images from wild type and *pi4kβ1 pi4kβ2* seedlings, as indicated. Scale bars, 10 μm. (b-d) Quantification of microtubular density (b), microtubular bundling (c) and microtubular velocity (d). Data represent mean ± SD. n.s., not significant ( $p > 0.05$ ) according to a two-tailed Student's *t*-test (wild type,  $n = 19$  cells; *pi4kβ1 pi4kβ2*,  $n = 12$  cells). \*, a significant ( $p < 0.05$ ) difference according to a two-tailed Student's *t*-test (\*  $p < 0.05$ ). For growth rate quantification in (d), wild type,  $n = 84$ ; *pi4kβ1 pi4kβ2*,  $n = 79$ ; for shrinkage quantification in (d), wild type,  $n = 68$  for, *pi4kβ1 pi4kβ2*,  $n = 53$ .



**Appendix Figure S9. Mislocalization of immunodetected GFP-MAP65-3 in cytokinetic root cells of Arabidopsis wild type controls and the *pi4kβ1 pi4kβ2* double mutant.** Immunofluorescence of a GFP-MAP65-3 marker (green) and microtubules (red), costained with DAPI (blue). MAP65-3 labeled the whole cell plate at late cytokinetic stages in five-day-old seedlings. The pattern is representative for > 40 cells for each genotype. Scale bars, 10  $\mu$ m.



**Appendix Figure S10. No effects of MPK4-mediated phosphorylation on in vitro activity or in vivo localization of Arabidopsis PI4Kβ1.** Based on the notion that PI4Kβ1 can be a target for phosphorylation by MPK4, experiments were performed to test whether this modification would influence activity or localization of PI4Kβ1. (a) In vitro phosphorylation of PI4Kβ1 by MPK4. Purified recombinant MPK4 was preactivated in the presence of MKK6<sup>DE</sup>, and the activated MPK4 was incubated with purified GST-PI4Kβ1 in the presence of  $\gamma$ -[<sup>32</sup>P]ATP. Proteins were separated by SDS-PAGE, and the incorporation of the radiolabel was analyzed by phosphor imaging. About 0.3  $\mu$ g MPK4, 0.2  $\mu$ g MKK6<sup>DE</sup>, 3  $\mu$ g GST-PI4Kβ1 and 3  $\mu$ g GST were employed, respectively. The experiment was performed once, and similar results were obtained when using maltose-binding protein-tagged PI4Kβ1 (MBP-PI4Kβ1) as a substrate (data not shown). Solid arrowhead, GST-PI4Kβ1; open arrowhead, GST-MPK4 and GST-MKK6<sup>DE</sup>. (b) Phosphorylation of PI4Kβ1 has no effect on PI4Kβ1 activity in vitro. Recombinant GST-PI4Kβ1 protein was preincubated with preactivated MPK4 by of MKK6<sup>DE</sup>, and subsequently analyzed for catalytic activity against the lipid substrate, PtdIns. The data represent the mean  $\pm$  SD from two experiments, each performed in triplicates. (c) Localization of mCherry-PI4Kβ1 is not altered in the Arabidopsis *mpk4-2* background. Four-day-old roots of *mpk4-2* plants expressing the functional mCherry-PI4Kβ1 were subjected to immunostaining using anti-mCherry (green) and anti-ARF1 (red) antisera, counterstained by DAPI (blue). mCherry-PI4Kβ1 localization was unchanged and could be observed at the cell plate in *mpk4-2* mutants. Images are representative for  $\geq 6$  cells for each stage. Scale bars, 10  $\mu$ m.

**Appendix Table S1. Genetic interaction between *PI4Kβ* and *MPK4* from *Arabidopsis*.** The genotypes of 181 progeny of self-pollinated *pi4kβ1*<sup>(-/-)</sup> *pi4kβ2*<sup>(+/-)</sup> *mpk4-2*<sup>(+/-)</sup> were determined by PCR. Expected values were calculated using Mendelian law. The p-value was calculated by chi-squared test. An asterisk indicates a significant difference from the expected number.

Genotype	Number observed	Number expected
<i>pi4kβ1</i> <sup>(-/-)</sup> <i>pi4kβ2</i> <sup>(+/-)</sup> <i>mpk4-2</i> <sup>(+/-)</sup>	35 (19%)	11 (6%)
<i>pi4kβ1</i> <sup>(-/-)</sup> <i>pi4kβ2</i> <sup>(+/-)</sup> <i>mpk4-2</i> <sup>(+/+)</sup>	19 (10%)	23 (13%)
<i>pi4kβ1</i> <sup>(-/-)</sup> <i>pi4kβ2</i> <sup>(-/-)</sup> <i>mpk4-2</i> <sup>(+/+)</sup>	11 (6%)	11 (6%)
<i>pi4kβ1</i> <sup>(-/-)</sup> <i>pi4kβ2</i> <sup>(+/-)</sup> <i>mpk4-2</i> <sup>(+/-)</sup>	54 (30%)	23 (13%)
<i>pi4kβ1</i> <sup>(-/-)</sup> <i>pi4kβ2</i> <sup>(+/-)</sup> <i>mpk4-2</i> <sup>(+/-)</sup>	20 (11%)	46 (25%)
<i>pi4kβ1</i> <sup>(-/-)</sup> <i>pi4kβ2</i> <sup>(-/-)</sup> <i>mpk4-2</i> <sup>(+/-)</sup>	9 (5%)	23 (13%)
<i>pi4kβ1</i> <sup>(-/-)</sup> <i>pi4kβ2</i> <sup>(+/+)</sup> <i>mpk4-2</i> <sup>(-/-)</sup>	29 (16%)	11 (6%)
<i>pi4kβ1</i> <sup>(-/-)</sup> <i>pi4kβ2</i> <sup>(+/-)</sup> <i>mpk4-2</i> <sup>(-/-)</sup>	4 (2%)	23 (13%)
<i>pi4kβ1</i> <sup>(-/-)</sup> <i>pi4kβ2</i> <sup>(-/-)</sup> <i>mpk4-2</i> <sup>(-/-)</sup>	0 (0%)	11 (6%)
Total number	181	-
p-value	-	2.49526E-33 <0.0001*